Synthesis and Characterization of Unsaturated Thermotropic Polyesters Prepared via Acyclic Diene Metathesis Polymerization

Haihu Qin,[†] Brian J. Chakulski,[‡,§] Ingrid A. Rousseau,[†] Jianzhong Chen,[†] Xiang-Qun Xie,[†,||] and Patrick T. Mather*[,†,‡]

Institute of Materials Science and Chemical Engineering Department, University of Connecticut, Storrs, Connecticut 06269

Gregory S. Constable and E. Bryan Coughlin

Department of Polymer Science and Engineering, University of Massachusetts, Amherst, Massachusetts 01003

Received February 5, 2004; Revised Manuscript Received April 25, 2004

ABSTRACT: Acyclic diene metathesis (ADMET) polymerization was employed to prepare thermotropic liquid crystalline polymers (TLCPs) bearing double bonds within flexible spacers. Starting from a diene monomer, 2-*tert*-butyl-1,4-phenyl bis(4-pentenyloxybenzoate) (5tB), we successfully synthesized unsaturated liquid crystalline oligomers and polymers, P5tB*n*, via ADMET polymerization. Such unsaturated TLCPs were developed to allow the preparation of tailored, thermally cross-linkable, liquid crystalline thermosets as adhesives and composite matrix resins. High degrees of polymerization were achieved and the resulting polymers showed clear mesomorphic behavior with complete absence of crystallization. Thermal analysis of polymers prepared with varying synthetic conditions showed that TLCPs prepared using different ruthenium metathesis catalysts featured substantially different transition temperatures, implying an influence of the catalyst on the resulting TLCP chain microstructure. In light of these observations, NMR studies (1D ^{1}H and ^{13}C, and 2D COSY and HMQC) were carried out, allowing determination of the selectivity of the catalysts toward trans/cis linkage and coupling/isomerization of units in the polymer chain. Furthermore, by studying the polymerization and isomerization kinetics, we shed light on the cause of isomerization. It was found that the degradation product of Grubbs catalyst is implicated in isomerization catalysis, in agreement with reports on the metathesis of 1-octene. In contrast, second-generation Grubbs catalyst itself (not a degradation product) apparently causes isomerization. For a related catalyst, developed by Nolan, both the catalyst and its degradation product are concluded to be responsible for the isomerization reaction.

Introduction

The incorporation of hydrocarbon or otherwise flexible spacers within the backbone of main chain liquid crystalline (LC) polymers has been an approach toward melting point depression and improved processing of such materials since their conception. In the area of main chain LC polyesters, several approaches toward spacer incorporation have been adopted, including copolymerization of semiflexible poly(ethylene terephthalate) (PET) with rodlike poly(4-hydroxybenzoic acid),[1] polycondensation of aliphatic dicarboxylic acids with mesogenic bisphenols,[2] and, especially, polycondensation of hydroquinones (substituted or not) with α,*ω*-bisbenzoic acids (such as 4,4′-dicarboxy-α,*ω*-diphenoxyhexane) bearing the spacer molecule.[3−6] Additionally, semiflexible polyethers with comparatively lower transition temperatures have been prepared from dibromoalkanes and mesogenic diols using a phase transfer catalyst approach.[7] Numerous studies of the phase behavior and physical properties of segmented liquid crystalline polymers (LCPs) have revealed the leading role of the spacer length, along with any mesogen pendent group, in determining crystallinity, phases observed, and phase transition temperatures. Perhaps the most intriguing aspect of studies, reviewed by Sirigu,[8] is the remarkable "odd−even" alternation in phase transition temperature(s) with increasing spacer length, indicating substantial conformational differences between segmented LCPs with an odd number of methylene spacer units (lower transition temperatures) and their even-numbered counterparts.

Despite the extensive work in the area of segmented LCP chemistry and physics, the field has been limited almost entirely to polymers formed by conventional polycondensation reactions, more particularly to polyesterifications wherein the mesogenic moiety is constructed during polymerization itself. As such, attainable molecular weights have been limited to those typical of polyesters (M_w < 30 000 g/mol) with great care required for stoichiometric balance in the AA/BB polycondensations. Additionally, functionalization of such polymers is not possible so that LCPs of this type have not been exploited in the areas of thermosets, adhesives, or reactive plasticizers. Instead, distinct small-molecule chemistry has been developed for such purposes,[9] often with significant compromise in toughness due to a lack of molecular entanglement.

The present work seeks to understand the preparation and properties of segmented LCPs polymerized by linking, via stepwise polymerization, separately prepared liquid crystalline dienes using metathesis chemistry. Acyclic diene metathesis (ADMET) polymerization, an application of the olefin metathesis reactions,

* Corresponding author. E-mail: patrick.mather@uconn.edu.
† Institute of Materials Science.
‡ Chemical Engineering Department.
§ Current address: UTC Fuel Cells, Hartford, CT.
|| Current address: College of Pharmacy, University of Houston, Houston, TX 77204.

10.1021/ma0497456 CCC: $27.50 © 2004 American Chemical Society
Published on Web 06/11/2004

Scheme 1. Schematic Representation of the Structure of the 5tB Diene Monomer and Its ADMET Polymerization To Form a Liquid Crystalline Polymer, P5tB

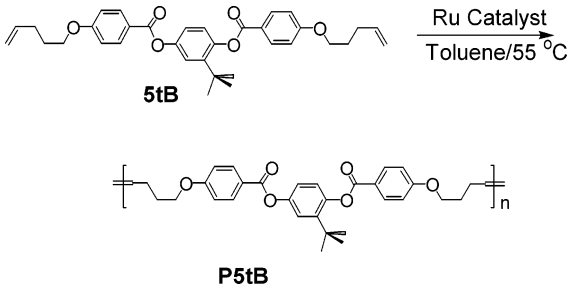

has been receiving increased attention since Wagener's pioneering work in the early 1990s.[10,11] Although ADMET polymerization bears some similarity to ring-opening metathesis polymerization (ROMP), these two reactions are mechanistically different. Specifically, while the chemical mechanism of ADMET requires two metallocyclobutane intermediates, only one is required in ROMP. Moreover, in each ADMET propagation step, the active metal species is released from the polymer chain, making ADMET a steplike condensation polymerization.[12] In contrast, ROMP polymerizations are of the chain-growth type, with each active metal species maintaining coordination with a single chain until a specific cleaving reaction occurs. Therefore, ADMET polymerization is less active and yields polymers with higher polydispersities than ROMP.

Noting that the range of cyclic monomers available for ROMP is quite limited, ADMET polymerization has the advantage of a broader range of possible polymer compositions and architectures. Indeed, in the past decade, a great variety of polymers, such as polyolefins,[12] polyethers,[13] polyesters,[14] polycarbonates,[15] polythioethers,[16] poly(carbosiloxanes),[17] as well as phosphazene-containing polymers[18,19] have been synthesized via ADMET polymerization. Most of the diene monomers in these polymerizations feature intricate structures unlikely to be available in a cyclic monomeric olefin for comparable ROMP polymerization. So far, there are only a few studies discussing the synthesis of LCPs via ADMET polymerization.[20,21] Importantly, ADMET polymers exhibit residual double bonds along their backbone available for further modification. For example, it was found that unsaturated polyethers could be cross-linked either by heat treatment or ultraviolet radiation.[22] Such double bonds could also be epoxidized up to 50% without apparent decomposition; however, the curing of such epoxidized polymers with hardeners has not been studied.

Here, we report on the ADMET polymerization of thermotropic liquid crystalline polymers (TLCPs), with specific attention given to the resulting chain microstructure and consequential thermal transition behavior. Specifically, we synthesized ADMET TLCPs from our newly synthesized monomer, namely 2-*tert*-butyl-1,4-phenyl bis(4-pentenyloxybenzoate) symbolized as 5tB (see Scheme 1), using Grubbs, Nolan's, and second-generation Grubbs (see Scheme 2) catalysts and studied the influence of the catalyst on the structures as well as the properties of the resultant LCPs using high-resolution NMR, in addition to gel permeation chromatography, differential scanning calorimetry, and hot-stage polarizing optical microscopy (POM).

Scheme 2. Schematic Representation of the Chemical Structures of the Three Ruthenium-Based Catalysts Used in Our Study: (i) Nolan's (N) Catalyst, (ii) Second-Generation Grubbs Catalyst (SG), and (iii) Grubbs Catalyst (G)

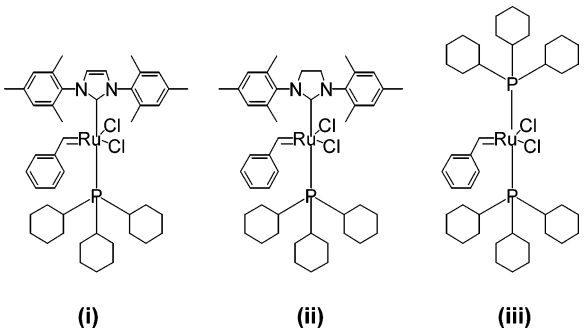

Experimental Section

Materials. The synthesis and the characterization of the monomer, 2-*tert*-butyl-1,4-phenyl bis(4-pentenyloxybenzoate), symbolized 5tB (Scheme 1), is described elsewhere.[23] The solvent for polymerization, toluene, was vacuum transferred over sodium and benzophenone and then stored in a dry glovebox. Nolan's catalyst (**N**) was generously donated by Prof. Nolan of the University of New Orleans. Grubbs (**G**) and second-generation Grubbs (**SG**) catalysts as well as tris-(hydroxymethyl)phosphine were purchased from Strem Co. Other chemicals and solvents were purchased from common commercial sources and used as received.

Polymerization, Postpolymerization, and Purification of the Polymers. By way of example, we provide one set of conditions and direct observations for the ADMET polymerization of P5tB-G2 (see Table 1), noting that variations from the procedure only involved changing the catalyst used, amount of solvent, and amount of catalyst or reaction time. In an inert gas-charged glovebox, 1.54 g (2.84 mmol) of 5tB monomer, 6 mL of anhydrous toluene, a magnetic stirrer bar, and 48 mg of **G** catalyst (0.058 mmol, [5tB]/[G] = 49) were mixed in a septum-sealed Schlenk flask. The flask was then removed from the glovebox and heated in an oil bath to 55 °C under magnetic stirring while argon was purged through the system. Upon stirring, the mixture quickly became homogeneous as a brownish purple solution (brownish red for the systems using **SG** or **N** catalysts) with evolution of a gas, presumably ethylene. As the reaction proceeded, the solution viscosity increased noticeably while the color of the polymerization solution became increasingly darker (eventually black), indicating catalyst degradation. After 6 h, the reaction was terminated (in this case) by first cooling to room temperature and then precipitating in 10-fold excess methanol. An overall schematic representation for this ADMET polymerization is given in Scheme 1.

The catalyst type and reaction time were varied in order to see their effect on molecular weight. Thus, polymer P5tB-N1 was prepared as above, but using 12.4 mg of **N** catalyst with 1.123 g of monomer in 1.5 mL of toluene ([5tB]/[N] = 141) and a reaction time of 24 h. For a targeted higher molecular weight, P5tB-N2 was obtained by polymerization initially with 0.30 g of monomer and 3.0 mg of **N** ([5tB]/[N] = 156) in 1 mL of toluene for 48 h total, with addition of 8.0 mg more of **N** in 0.5 mL of toluene occurring after 27 h. P5tB-SG1 was prepared using 0.85 g of 5tB and initially 50 mg of **SG** catalyst ([5tB]/[N] = 26.6) with another 50 mg of **SG** being added after 19 h. The whole polymerization lasted 64 h and fresh solvent was added to maintain a constant concentration of solids. P5tB-G1 was prepared using 0.50 g of 5tB with the same monomer and catalyst concentration as P5tB-G2 ([5tB]/[G] = 49) but a much longer reaction time of 66 h.

Postpolymerization was carried out with 0.32 g of P5tB−N1 and 11 mg of **SG** ([P5tB-N1]/[SG] = 10) in 1 mL of toluene. Later (25 h), an additional 7 mg of **SG** catalyst in 1.6 mL of toluene was added. The reaction lasted for a total of 96 h,

Table 1. Characteristics of the ADMET Polymers Obtained Using Various Catalysts

sample	catalyst[a]	$\bar{M}_n^{NMR}$ (kDa) (NMR)	$\bar{M}_n$ (kDa) (GPC)	PDI (GPC)	T_g (°C)	T_{NI} (°C)	% trans	% isomerization
P5tB-N1	N	3.9	2.8	1.50	64.2	184.6	78	10
P5tB-N2	N	10.1	10.3	1.80	73.8	194.7	78	12
P5tB-SG1	SG	[b]	15.4	1.47	74.1	170.0	[c]	29
P5tB-N/SG2[d]	N/SG	[b]	23.1	1.54	75.5	172.0	[c]	29
P5tB-G1	G	17.6	5.8	1.68	66.7	174.2	65	13
P5tB-G2	G	7.2	9.6	1.45	62.4	186.9	68	7

[a] N: Nolan's catalyst; SG: Second Generation Grubbs catalyst; G: Grubbs catalyst. [b] Not determined due to absence of specific terminal double bonds signal. [c] Not determined due to overlapping peaks. [d] Synthesized from the P5tB−N1 oligomer.

during which time vacuum was applied twice to remove ethylene from the system, with 2 mL of toluene added afterward to compensate for solvent loss. The sample is designated P5tB-N/SG2.

All of the polymeric products were first purified by precipitation in a 10-fold excess of methanol, leading to fibrous or powder-like solids after filtration, depending on molecular weight. The dried solids exhibited a light brownish color, indicative of residual ruthenium complexes that were subsequently removed by dissolving in $CHCl_3$ and washing with a 22% (w/v) solution of tris(hydroxymethyl)phosphine (THP) in 2-propanol, representing an excess of at least 22 molar equiv of THP per catalyst to be removed.[24] After stirring the solution vigorously under an inert atmosphere at 55 °C for 24 h, the polymer was precipitated from the solution with methanol, resulting in a white powder. For all reactions, the total yield after the two-step purification always reached values above 75%, despite of the inevitable loss of polymer during filtration.

Characterization. (i) Nuclear Magnetic Resonance (NMR). NMR spectroscopy was employed to investigate the molecular structure of our polymerization products, particularly the nature of the internal −C═C− double bonds along the TLCP backbone. Thus, high-resolution 1D and 2D NMR spectra were obtained on a Bruker AVANCE DMX500 spectrometer with a 5 mm inverse detection, triple resonance gradient probe and a BVT-2000 temperature controller. 1D 500 MHz ^{1}H NMR spectra were recorded using the following acquisition parameters: a 90° pulse width of 6.2 μs, a spectral width of 10 kHz (20 ppm), a data size of 32k, a 10 s recycling delay, and 16 transients. The 125 MHz ^{13}C spectra were performed with 90° pulses of 14.5 μs, a spectral width of 43750 Hz (350 ppm), a data size of 64k, a 2 s recycling delay, and a number of transients of 8k. 2D phase-sensitive ^{1}H−^{1}H COSY spectra (DQF-COSY) were recorded with a recycling delay of 2 s at a temperature of 298 K. The data sizes were 512k in F_1 and 2k in F_2 and were zero-filled in F_1 prior to 2D Fourier transformation to yield a 2k × 2k data matrix. The spectra were processed using a Qsine-bell window function in F_1 and F_2. 2D ^{1}H−^{13}C inverse correlated experiments with heteronuclear multiple quantum coherence (HMQC) were performed using an inverse detection probe with a delay time of 3.57 ms for the J_{C-H} value and a delay of 0.35 s for bilinear rotation decoupling (BIRD) inversion pulse. 2D ^{1}H−^{13}C inverse correlated experiments with heteronuclear multiple bond correlation (HMBC) were conducted using similar acquisition parameters as for HMQC, while a proper delay time (50 ms) was chosen to enhance the observation of selected long-range couplings (e.g., $^2J_{C-H}$, $^3J_{C-H}$, and $^4J_{C-H}$).

(ii) Gel Permeation Chromatography (GPC). Gel permeation chromatography (GPC, Waters Associates, 150-C Plus) with a PL-ELS 1000 control detector (Polymer Laboratories) was used to obtain molecular weights (MWs) and molecular weight distributions (MWDs) of the ADMET TLCPs. Samples were dissolved in THF at a concentration of about 0.1 wt % and injected at 35 °C with THF as the eluent at a flow rate of 1.0 mL/min. GPC data reported for the MWs and MWDs of the synthesized TLCPs are relative to a calibration based on monodispersed polystyrene standards (472, 982, 4000, 6930, 43 000, 200 000, 400 000, and 824 000 g/mol; Polymer Standards Service-USA, Inc.).

(iii) Thermal Analysis. The thermal behavior of the ADMET TLCPs was evaluated by differential scanning calorimetry (DSC) measurements performed on a TA Instruments DSC2910 under nitrogen. Samples weighing approximately 5 mg were first heated to 220 °C at 10 °C/min to erase thermal history, quenched to 0 °C, and finally heated at 10 °C/min to an upper temperature limit that depended on the nature of the experiment (see Results). This second heating trace is that used for discussion of the thermal behavior.

(iv) Polarized Optical Microscopy (POM). Liquid crystalline textures and thermal transitions of the TLCPs were investigated using hot-stage POM. Samples were prepared after initial degassing in a vacuum oven by pressing into thin films between two glass cover slips at 150 °C in their liquid crystalline state. After quenching to room temperature, the samples were then heated to 150 °C at 5 °C/min, annealed for 10 min, and then cooled to 30 °C at 5 °C/min. This intermediate annealing step was incorporated into the protocol in order to coarsen the TLCP texture, thereby reducing turbidity and allowing sufficient light transmission for phase identification. POM was conducted using an Olympus BX50 microscope equipped with a CCD camera (Panasonic GP−KR222) and a temperature-controlled hot stage (Instec STC 200) operated with a ramping rate of 5 °C/min. The samples were observed between crossed polarizers, allowing imaging of the local retardance convolved with orientation angle according to eq 1,

$$\frac{I}{I_o} = \sin^2\left(\pi\frac{\Delta nh}{\lambda}\right)\sin^2(2\chi) \qquad (1)$$

where Δnh is the retardance, λ is the wavelength, and χ is the angle between the local nematic orientation and the polarizer. A long working distance objective lens of 50× power and a numerical aperture of 0.2 was used.

(v) Wide-Angle X-ray Diffraction (WAXD). To aid in phase identification of the synthesized TLCPs by POM and DSC, WAXD patterns of selected samples were collected in reflection mode using a Bruker AXS D5005 powder diffractometer operated with a Cu Kα source (λ_{X-ray} = 1.5418 Å) operating at 40 kV and 40 mA. Reflection data were collected over the range 3° < 2θ < 50° (1.824 Å < d-spacing < 29.45 Å) on samples held at room temperature in a vitrified state.

Result and Discussion

(i) Polymerization and Purification. Factors Affecting Molecular Weight. ADMET polymerization of the 5tB monomer lead to polymers with number-average molecular weights, $\bar{M}_n$, ranging from 2800 to 15 400 Da, depending on the reaction conditions and catalyst employed. The sample names and catalyst used, along with measured molecular weights, polydispersities, transition temperatures (T_g and T_{NI}, described later), trans/cis ratio, and degree of isomerization (also described later) are compiled in Table 1. The first two polymers, namely P5tB-N1 and P5tB-N2, were catalyzed by **N** catalyst under distinct conditions and found to feature quite different number-average molecular weights (GPC) of 2.8 and 10.3 kDa. The higher value for P5tB-N2 is attributed to a combination of the higher monomer/catalyst mole ratio used and the second ad-

dition of catalyst during the reaction. P5tB-SG1, polymerized using the **SG** catalyst, was characterized by a higher molecular weight of 15.4 kDa. P5tB-G1 and P5tB-G2 resulted from nominally identical polymerization conditions with the **G** catalyst and were found to feature number-average molecular weights of 5.9 and 9.6 kDa for polymerization times of 66 and 6 h, respectively. This finding is attributed to intrinsic batch to batch variability in the molecular weights rather than a specific time effect, as kinetic studies will later show early saturation of molecular weight for **G**-catalyzed polymerization of 5tB. Indeed, systematic study of the effects of catalyst on polymerization, including the molecular weight, will be presented in reference to Figure 7.

As mentioned in our introductory remarks, ADMET polymerization follows a stepwise polymerization mechanism[25] and, therefore, should result in polydispersities (M_w/M_n) of approximately 2. However, our results (see Table 1) indicate distributions with lower polydispersities closer to 1.5. We attribute this finding to a nondeliberate fractionation that occurs during the multiple step purification of the polymers. Specifically, we postulate that our purification procedure removes the lower molecular weight portion of the as-polymerized molecular weight distribution.

Even in light of the high vapor pressure of its ethylene byproduct, the reversible nature of the ADMET polymerization of 5tB demands purging of the reactor, removing the evolved ethylene formed, so that the reaction equilibrium favors polymerization. Moreover, the ADMET catalysts employed are somewhat sensitive to traces of impurities, especially water and oxygen, so that degradation of the catalyst may also occur during polymerization. As a result, the attainable molecular weight actually depends on polymerization conditions such as catalyst concentration, monomer concentration, reaction time, and reactor purging rate. Nevertheless, the resulting polymers should be end-capped with vinyl groups and, therefore, still be "alive" for further ADMET polymerization.

We tested the ability to polymerize further by exposure of such polymeric products to fresh catalyst, finding that indeed polymerization can be advanced in this way. For example, the secondary polymerization of P5tB-N1 (prepared with **N**) utilizing the **SG** catalyst yielded P5tB-N/SG2 with a final postpolymerization molecular weight of 23.1 kDa, a dramatic increase of the P5tB-N1 2.8 kDa value. This finding provides solid evidence for the persistent reactivity of polymers from ADMET polymerizations. Additionally, this finding suggests a practical way to control the molecular weight of the homopolymers as well as to construct copolymers with different architectures, such as multiblock copolymers, triblock copolymers, and telechelics.

Impact of Catalyst Removal. Initial investigations of the TLCP phase behavior revealed sensitivity to the existence of remaining catalyst. Here we describe example results for the **SG**-catalyzed system, although the findings were virtually the same for other catalysts. Figure 1 shows (i) the first heating DSC to 220 °C, (ii) the first cooling to 0 °C, and (iii) the second heating to 350 °C for P5tB-SG1 before (graph **a**) and after (graph **b**) catalyst removal with THP (see Experimental Section). Despite a lack of baseline stability present in the first heating step (traces i in both graphs **a** and **b**), that we attributed to the thermal histories, each of the DSC

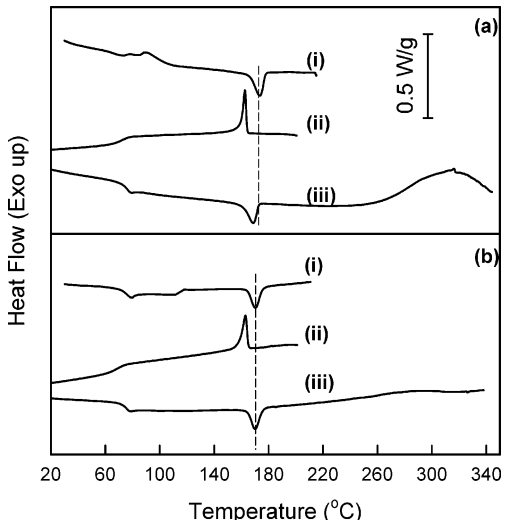

Figure 1. DSC traces of P5tB-SG1 before (a) and after (b) catalyst removal. The DSC traces of first heating to 220 °C (i), first cooling to 0 °C (ii), and second heating to 350 °C (iii) are presented in each plot. The ramping rates are of 10 °C/min for all the traces.

traces still clearly shows a glass transition around 75 °C and a first-order transition around 170 °C. Together with POM studies, which will be discussed in detail later in this paper, we deduce that this peak corresponds to the nematic to isotropic transition. From Figure 1a, we can see that without catalyst removal heating the samples to $T = 220$ °C results in a significant decrease in the clearing point, as evidenced by the second heating trace (from 173.6 °C during first heating to 168.6 °C during second heating). Moreover, at higher temperatures (≥250 °C), a significant and broad exothermic peak is observed, centered at $T = 320$ °C, indicating that additional reactions occur. Most importantly, as a result, the samples became insoluble in organic solvents. On the basis of these observations, we conclude that the exothermic peak is related to cross-linking of the unsaturated polymers. However, the mechanism of cross-linking and explanation for the decrease of the clearing point is the subject of continuing investigation.

After the removal of the catalyst by treatment with THP, we observe the stability of the LCP phase behavior to improve dramatically. In Figure 1b, the nematic-to-isotropic transition remains constant (170.0 °C) throughout the first and second heating traces. Additionally, no significant exotherm that would suggest subsequent chemical cross-linking is evident. This finding was corroborated by an observation that samples could be completely dissolved (i.e., negligible gel fraction) in chloroform after the DSC experiments. Despite the major differences found regarding the stability of the TLCP phase behavior due to catalyst removal, simple ^{1}H NMR and FTIR analyses showed no major differences in as-synthesized chain composition, whether the catalyst was removed or not. In the light of this finding, the DSC and POM characterizations of P5tB*n* polymers were conducted after catalyst removal using the described protocol.

(ii) Chain Microstructure. To quantitatively confirm the polymer structure drawn in Scheme 1, we have employed 2D liquid-phase NMR methods as described in Experimental Section. The spectral assignments for the P5tB*n* polymers were made initially by an analysis based on chemical shifts. Subsequently, they were

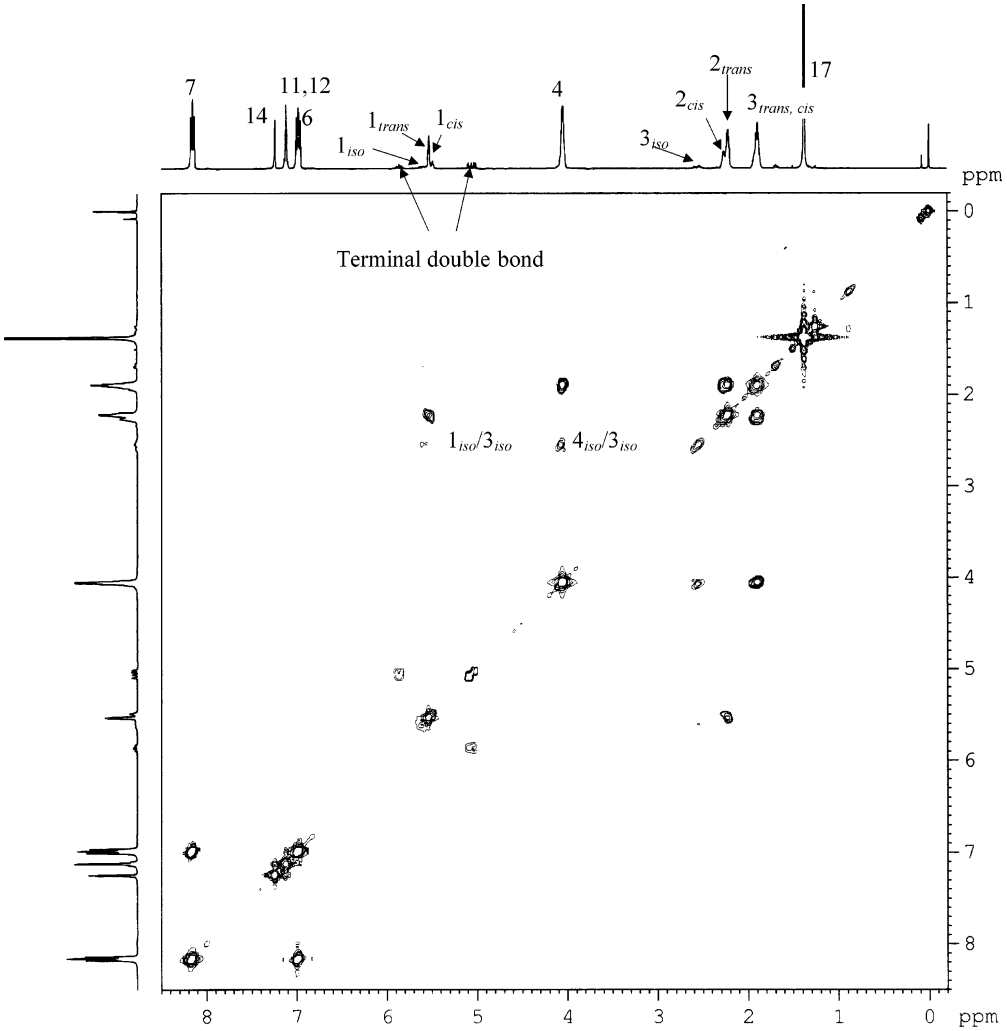

Figure 2. 2D $^1H-^1H$ DQF-COSY spectrum of P5tB-N1 in $CDCl_3$ at 298 K. The polymerization was catalyzed using **N** catalyst (M_n = 2.8 kDa). The proton at 2.54 ppm is coupled both with the proton in the methoxy group (4.07 ppm) and the proton in the internal double bond (5.59 ppm), arising from the isomerization reaction.

specifically assigned on the basis of their coupling connectivities as seen in the $^1H-^1H$ DQF-COSY (see Figure 2), $^1H-^{13}C$ HMQC (see Figure 3), and HMBC spectra (not shown). The aromatic protons were first assigned by analogy with monomers and then confirmed by analyzing the results of the 2D COSY experiment. The *tert*-butyl group protons can be readily distinguished by integration. For the remaining protons, a logical starting point is the H-4 proton (see Scheme 3), which was assigned at 4.06 ppm by analogy with the monomer. The protons H-3 (1.90 ppm), H-2 (2.22 ppm), and H-1 (5.53 ppm) were readily assigned from the couplings in the DQF-COSY spectrum, while carbons C-4, C-3, C-2, and C-1 were assigned to the chemical shifts 67.88, 28.70, 28.84, and 130.88 ppm, respectively, after identifying the $^2J_{H-C}$ coupling in the HMQC spectrum. We have assigned the two small peaks at 2.26 and 5.49 ppm in the 1D ^1H spectra (Figure 2, top) to be H-2 and H-1 in the cis double bond conformation, although this assignment is not unambiguous. By analogy with the monomer, the protons on the terminal double bond of the polymer main chain were assigned to 5.86 and 5.05 ppm, which was confirmed by the integration ratio of the peaks in the 1D proton spectrum and $^3J_{H-H}$ coupling in the DQF-COSY spectrum. In addition, multiple peaks at 2.54 ppm were found to correspond to the H-3 chemical shift by identifying the $^3J_{H4-H3(iso)}$ coupling in the DQF-COSY spectrum in the iso double bond structure as described in detail in section iv, below. The complete assignments of proton and carbon chemical shifts are summarized in Table 2, while the labeling of the atoms and the structure of the polymer are shown in Scheme 3.

In addition to the chain microstructure discussed above, ^1H NMR studies (Figure 4) allowed for the determination of the number-average degree of polymerization ($\overline{DP_n}$) and thus the number-average molecular weight (M_n^{NMR}) for those polymers featuring relatively low molecular weight. Specifically, the signals characteristic of the vinyl end groups (at 5.05 and 5.86 ppm) of the ADMET polymers are apparent in the ^1H NMR (Figure 4b). Therefore, $\overline{DP_n}$ can be estimated from the peak area ratio of the internal double bond protons (at 5.53 ppm) to the terminal double bond protons (at 5.05 ppm) following

$$\overline{DP_n} = \frac{A_i}{A_t} \times f \qquad (2)$$

Here, A_i and A_t represent the peak areas of the internal (5.53 ppm) and terminal double bonds (5.05 ppm). The factor f is the number of terminal double bonds per polymer chain, which was taken as 2, i.e., the case of

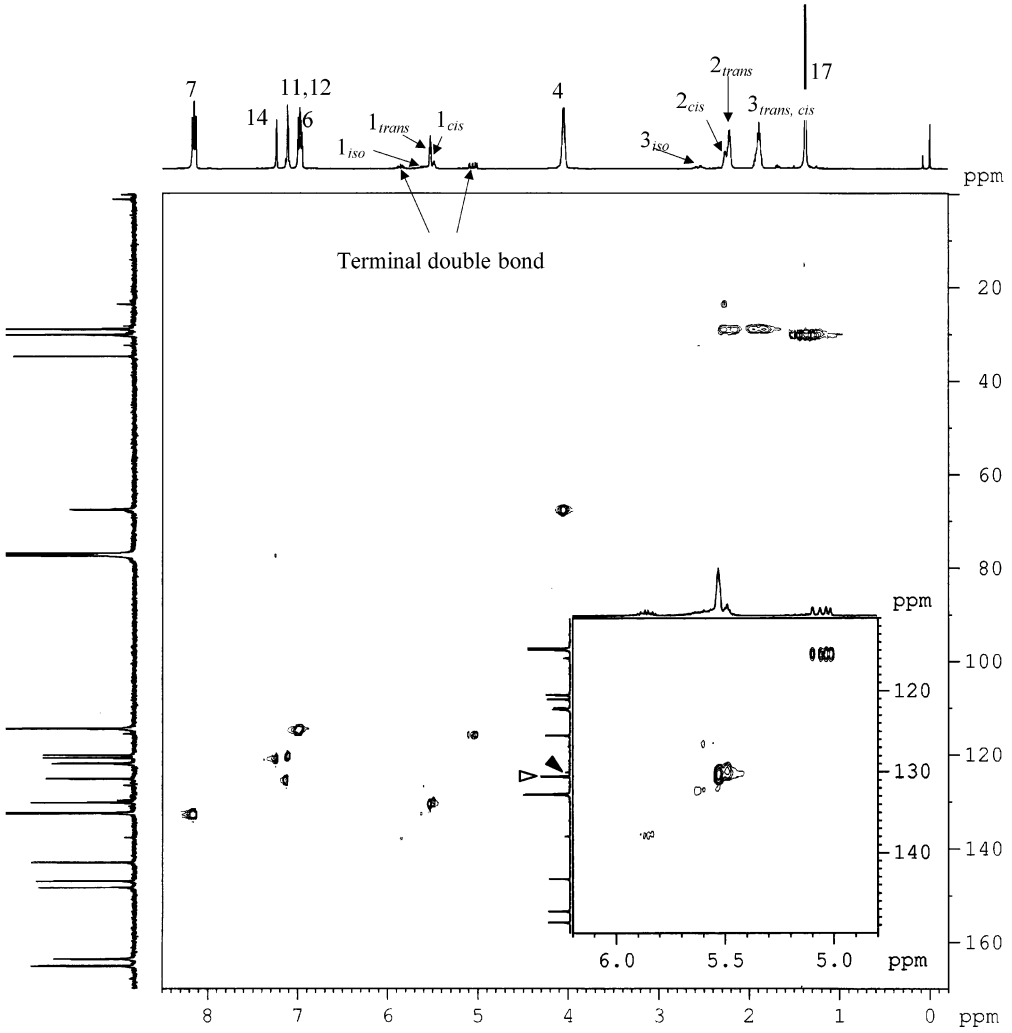

Figure 3. 2D $^{1}H-^{13}C$ HMQC spectrum of P5tB-N1 in $CDCl_3$ at 298 K. The polymerization was catalyzed using **N** (M_n = 2.8 kDa). Enlargements of areas b (double bonds area) and c (alkyl spacer area) are shown for clarity. The carbons from the trans double bonds give a signal at 130.88 ppm (open arrowhead) and the cis carbons give a signal at 130.07 ppm (filled arrowhead). In the ^{1}H NMR, the peak at 5.50 ppm is coupled with the cis carbon, while the peak at 5.54 ppm is coupled with the trans carbon. The ^{13}C at 23.51 ppm was assigned to the end group as determined by the COSY and HMQC results.

ideal ADMET polymerization. Knowing the mass of each repeat unit, the number-average molecular weights were calculated and are reported in Table 1, revealing reasonable comparison with the data from GPC that utilized polystyrene standards. Also discernible in Figure 4c are the peaks at 2.54 ppm, which correspond to the isomerized structures, as we will discuss in detail in section iv below.

(iii) Phase Behavior of the Polymers. Liquid crystalline phase behavior was observed with DSC, POM, and WAXD studies, revealing that all P5tB*n* polymers featured a simple nematic glass → nematic liquid → isotropic liquid phase sequence on heating, though with sensitivity of the transition temperatures to the polymerization catalyst employed. Figure 5 shows the heating traces of three samples (P5tB-N2, P5tB-SG1, and P5tB-G2) synthesized using **N**, **SG**, and **G** catalysts, respectively. Each of the DSC traces shows a glass transition (T_g) around 70 °C and an endothermic peak ranging from 170 to 195 °C. Combining these results with the hot stage POM observations and the absence of either smectic- or crystalline-type WAXD reflections (data not shown), we attribute the endothermic peak to the nematic-to-isotropic transition. As an example, a sequence of POM micrographs for P5tB-SG1 is shown in Figure 6. At low temperatures such as 30 °C, a fine nematic texture is observed. During the course of the heating, texture coarsening is initiated when the temperature exceeds T_g, leading to a comparatively coarse structure at 165 °C. With continued heating, the nematic-to-isotropic transition (T_{NI}) occurs over the temperature range 168 °C < T < 174 °C, a finding in good agreement with the result of DSC (curve i in Figure 5), where the endothermic T_{NI} peak was observed at 170 °C. Upon cooling, the nematic phase reemerges at T = 166.7 °C, quickly nucleating disclinations that are slow to coarsen for such a molecular weight ($\bar{M}_n$ = 15.4 kDa, Table 1). Thus, the darkness of the POM micrographs for T = 161 °C and T = 133 °C is attributed to significant multiple scattering of light away from the path of the objective lens collecting the light for microscopy. Prolonged annealing of samples near T = 160 °C after such a clearing cycle (nematic → isotropic → nematic) was capable of coarsening to brighter nematic textures as bright as the ones observed on heating to T = 168 °C, for example.

The presence of the bulky *tert*-butyl group apparently suppresses crystallization, as was found previously for

Scheme 3. Structure of the Polymer (P5tB) and Itemization of the Structures of trans, cis and Isomerized Repeat Units in the Polymer[a]

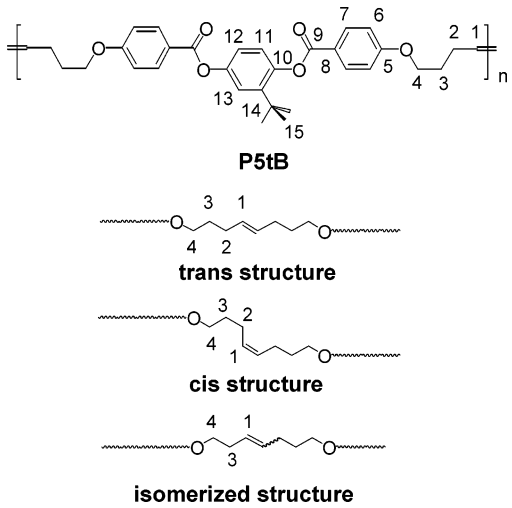

[a] The numbers are meant to indicate both the carbons and the protons thereon. In the isomerized unit, one methylene group (carbon 2 and protons thereon) is missing.

Table 2. ^{1}H NMR (500 MHz) and ^{13}C NMR (125 MHz) Chemical Shift Assignments for the Polymers Obtained by ADMET Polymerization[a]

H and C label	^{1}H (δ, ppm)	^{13}C (δ, ppm)	H and C label	^{1}H (δ, ppm)	^{13}C (δ, ppm)
1 trans-	5.53	130.88	9		165.46
1 cis-	5.49	130.07	10		146.78
1 iso-	5.59	132.58	11	7.12	120.02
2 trans-	2.22	28.84	12	7.12	126.41
2 cis-	2.26	23.51	13		148.16
3 trans-, cis-	1.90	28.70	14	7.23	120.56
3 iso-	2.54	32.35	15		142.82
4	4.06	67.88	16		34.69
5		163.37	17	1.38	30.05
6	6.98	114.44	18		163.40
7	8.16	132.27	end group	5.86 (1H)	137.95
8		164.96	(terminal double bond)	5.05 (2H)	115.95

[a] The labeling of the hydrogen and carbon atoms is shown in Scheme 3.

another segmented LCP bearing the same group.[6] Therefore, no melting or crystallization transitions were detected by either DSC or POM. We note that this amorphous (albeit liquid crystalline) nature of the polymer actually facilitates polymerization to high molecular weight since, if the polymer were crystalline, the oligomers would have precipitated from the reaction system, thus preventing further polymerization.[26] Moreover, the absence of crystallization offers a quite broad nematic range for the TLCPs—greater than 100 °C—that will facilitate fundamental study of TLCP physical properties.

It is well-known that nematic-to-isotropic transition temperatures for TLCPs are influenced by the molecular weight of the polymer. For example, Kim et al.[27] found that the higher the molecular weight of their LCP, PSHQ10, the higher the transition temperature. As our results indicate in Table 1, our liquid crystalline polymers also follow this trend. For instance, in the case of the two samples obtained using **N** catalyst (P5tB-N1 and P5tB-N2), both T_g and T_{NI} of the higher molecular weight sample (10.3 kDa) occur 10 °C higher than those of the lower molecular weight sample (2.8 kDa). However, in Figure 5 we notice that polymers of similar molecular weight but obtained via different catalysis routes were not comparable in terms of their T_g and T_{NI} temperatures. The ordering of T_{NI} values was found, for similar molecular weights, to follow the ranking **N** (195 °C) > **G** (187 °C) > **SG** (170 °C). To understand the origin of this important observation, we again employed liquid-phase NMR methods, this time to reveal more subtle differences in chain architecture.

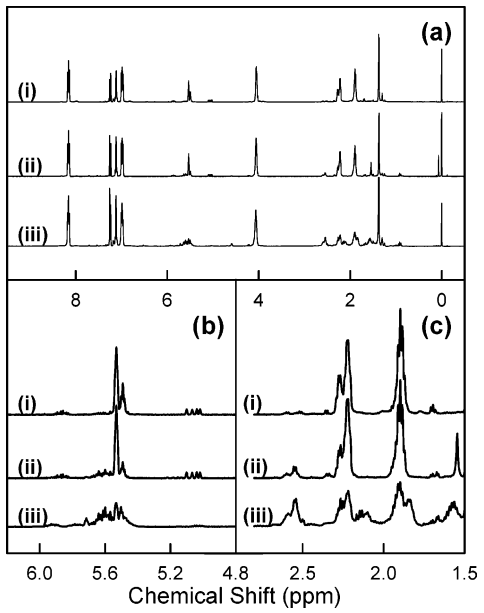

Figure 4. The full (a), double bonds region (b), and alkyl region (c) of the ^{1}H NMR spectra of (i) P5tB-G1 using **G** catalyst, (ii) P5tB-N2 using **N** catalyst, and (iii) P5tB-SG1 using **SG** catalyst. The assignment (see Table 1) was made on the basis of the results of ^{1}H−^{13}C (HMQC) and ^{1}H−^{1}H (COSY) spectra, as explained in the discussion section of this report.

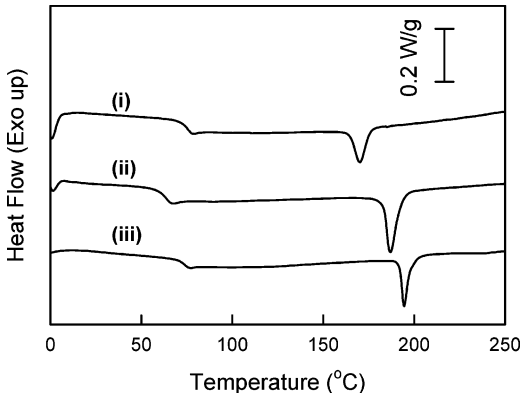

Figure 5. DSC heating traces (10 °C/min) of P5tB*n* obtained by ADMET polymerization with different catalysts: (i) **SG** (P5tB-SG1); (ii) **G** (P5tB-G2), and (iii) **N** (P5tB-N2). Samples were first heated to 220 °C and then cooled to 0 °C at 10 °C/min before the heating data shown were collected.

(iv) Chain Microstructure Influence on Material Phase Behavior. As mentioned above, DSC shows that the polymers obtained using different catalysts have different transition temperatures. For the P5tB-N2 sample (**N**), the T_g and T_{NI} are 73.8 and 194.7 °C, respectively. By comparison, P5tB-SG1 (**SG**) and P5tB-G2 (**G**) exhibit T_g at 74.1 and 62.4 °C and T_{NI} at 170 and 186.9 °C, respectively. These variations in glass transition and nematic-to-isotropic transition temperatures were not initially expected due to the fact that

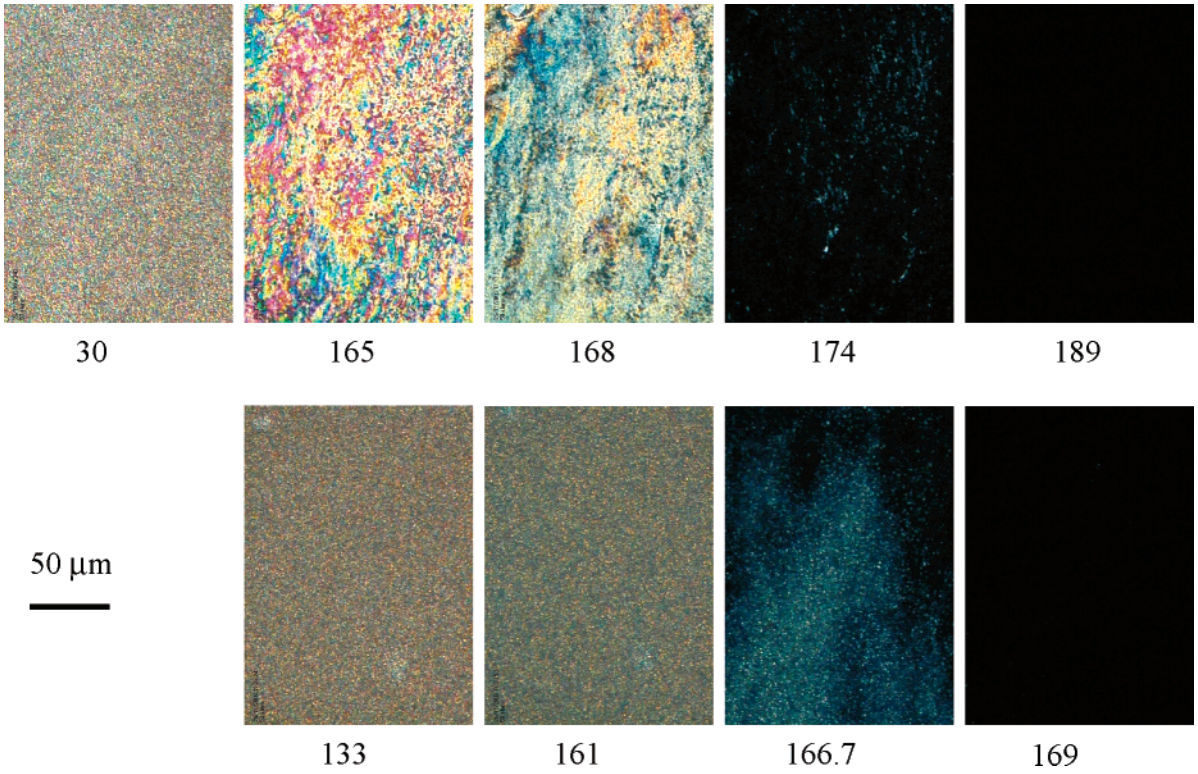

Figure 6. Polarized optical microscopy (POM) pictures of P5tB-SG1 (obtained using **SG** catalyst) between crossed polarizer and analyzer. The top pictures were taken during heating at 5 °C/min. The bottom pictures were obtained during cooling at 5 °C/min. The scale bar on the left represents 50 μm. The temperature (°C) at which each picture was taken is showed below each micrograph.

the molecular weights of these three samples were relatively close to each other (10.3, 15.4, and 9.8 kDa). Furthermore, the sample with the highest molecular weight, P5tB-SG1, actually exhibits the lowest clearing point, a tendency that cannot be explained by the molecular weight effect alone. Hence, we suspected that the different catalysts give rise to varying polymer structures and thus, different transition temperatures.

While Scheme 1 shows the polymer chain structures expected to result from ADMET polymerization of the 5tB monomer, one can quickly observe that there is ambiguity with respect to the trans/cis configuration of the carbon−carbon double bond coupling the repeating units. Additionally, it is known that ruthenium catalysts of the type used in this study are capable of isomerizing alkenes,[28,29] so that we envisioned possible competition between isomerization and coupling for each reaction step and the possibility of an isomerization−coupling sequence that would yield a shorter spacer length in the polymers. With regard to the first microstructural detail, it was previously demonstrated that the melting point, T_m, of semicrystalline poly(octenylene) polymerized via tungsten-catalyzed ROMP was affected by its trans/cis ratio, following the expression known as Calderon's equation,[30]

$$\frac{1}{T_m} - \frac{1}{T_m^0} = -\frac{R}{\Delta H_m} \ln N_T \qquad (3)$$

where N_T is the mole fraction of trans conformers, R is the universal gas constant, and ΔH_m and T_m^0 are the melting enthalpy and temperature for the limiting all-trans polymer. Thus, the melting point of this polymer increases systematically with trans content. Similarly, Wagener et al.[12] showed that the melting points obtained for poly(octenylene) synthesized via ADMET polymerization of 1,9-decadiene also followed Calderon's equation, at least for the range of N_T values spanning 0.77−0.93. On the basis of these prior observations, we hypothesized that a similar influence of *trans/cis* conformer ratio might exist for TLCP clearing temperature, T_{NI}, and each catalyst would yield a unique transition temperature dictated by the trans/cis ratio.

Regarding isomerization versus coupling, there are several reports on the selectivity of metathesis catalysts toward or against isomerization. Among the catalysts shown in Scheme 2, Dinger[31] demonstrated that **G** (Scheme 2 (iii)) exhibited an excellent selectivity against isomerization (less than 1% for 1-octene) while **N** (Scheme 2, i) led to a degree of isomerization as high as 15%,[32,33] during ring-closing metathesis reactions. When Lehman et al.[34] studied the selectivity of **SG** in metathesis reactions of 1-octene as well as other alkenes, an increased degree of isomerization was observed over that of **G**. Indeed, the metathesis of a 1 M solution of 1-octene in THF led to only 21.8% of desired metathesis product, tetradecene, while the major isomerization product, tridecene, accounted for 23.0% of the final product.[35]

Thus, the trans/cis ratio of the spacer double bonds and the degree of isomerization prior to coupling are considered to be variable for our polymerizations and important in determining physical properties. In Scheme 4, structures resulting from both coupling and sequential isomerization−coupling are shown. To determine the trans/cis ratio and the degree of isomerization versus coupling, a variety of NMR techniques, such as 2D ^{1}H−^{1}H (COSY) and 2D ^{1}H−^{13}C NMR heteronuclear correlation (HMQC, HMBC), as well as the ordinary 1D ^{1}H and ^{13}C NMR spectroscopy techniques, were used allowing peak assignment for protons and carbons in the different double bond configurations or isomerized

Scheme 4. Schematic Representation of the Synthetic Routes Available to ADMET Polymerization[a]

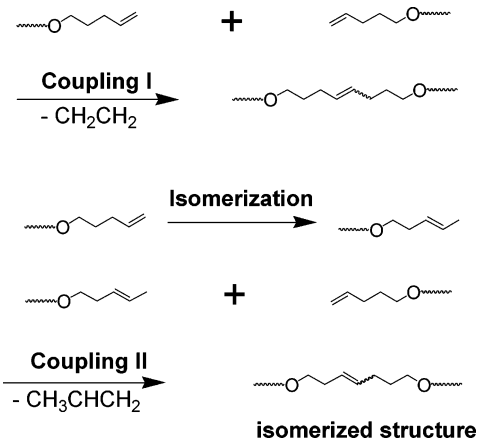

[a] The top scheme represents the polymerization of two nonisomerized terminal double bonds. The middle scheme shows the isomerization of a terminal double bond to internal double bond. The bottom scheme is the polymerization between an isomerized internal double bond and a terminal double bond, forming an isomerized structure in the polymer chain.

structures mentioned above in the Chain Microstructure section.

In the COSY spectrum (Figure 2), the multiple peaks at 2.54 ppm are coupled with the internal double bond protons at 5.59 ppm as well as with the methyloxy group protons at 4.07 ppm. We assigned this peak at 2.54 ppm to the methylene proton in the isomerized−coupled structure (Scheme 3, bottom), where it is next to both the double bond and the methoxy group (see Scheme 3, bottom, position 3). By comparing the peak area associated with the isomerized structure (2.54 ppm) to that associated with coupling (1.90 ppm), one can calculate the isomerization/coupling ratio resulting from ADMET polymerizations using different catalysts (Figure 4c). In doing so, we find that the selectivity of coupling to sequential isomerization−coupling follows the order **G** (93%)> **N** (90%) > **SG** (71%). Further comparison of the catalyst effect on isomerization is presented in the context of our kinetics study (Figure 7) below.

The HMQC spectrum (Figure 3, triangles) shows two peaks at 130.88 (open triangle) and 130.07 (filled triangle) ppm. We assign the peak at 130.88 ppm to the carbons of trans double bonds and the peak at 130.07 ppm to the cis carbons, which is consistent with Wagener's result for ADMET polymerization of 1,9-decadiene.[12] A close-up of the HMQC spectrum (Figure 3, inset) shows strong coupling between these two peaks and the peaks characteristic of the internal double bond protons at 5.53 and 5.49 ppm, revealing that the trans proton peak appears at 5.53 ppm and the cis proton at 5.49 ppm. This peak assignment now allows for the determination of the trans/cis ratio by ^{1}H NMR, which is much more convenient than its calculation from ^{13}C NMR. The results are shown in Table 1, where we see that, despite the attractive selectivity of **G** toward direct coupling, the same catalyst shows less selectivity toward the trans configuration (trans/cis = 68/32) than the **N** catalyst (78/22).

By comparing the rankings of trans/cis ratio and coupling−isomerization to the ranking of clearing temperatures (T_{NI}) depending on the catalyst used (Table 1), it is apparent that the trans/cis ratio plays a dominant role in dictating the clearing temperature.

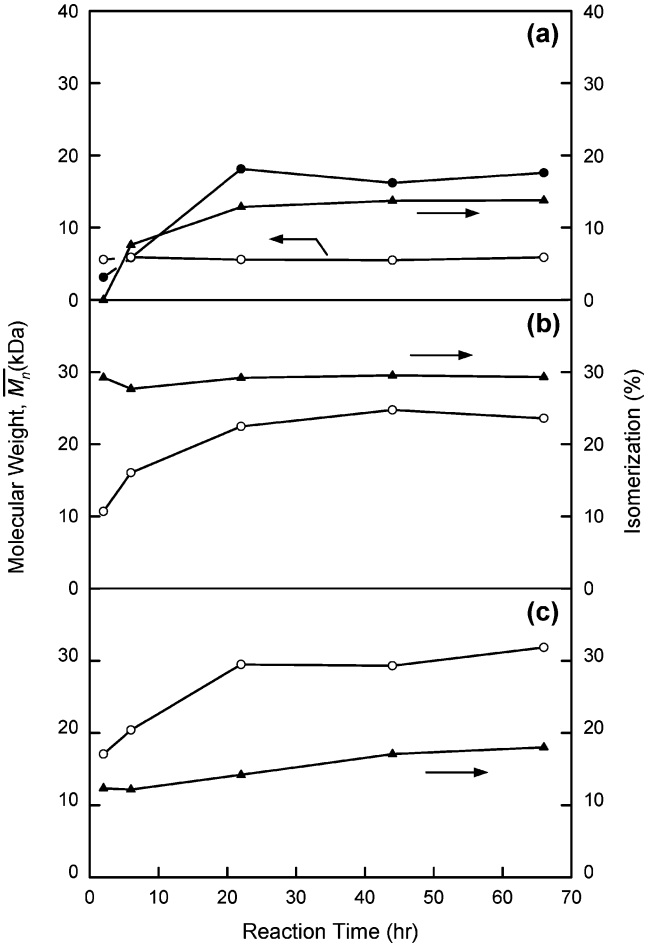

Figure 7. Kinetic studies of the polymerization and isomerization reactions catalyzed by: (a) **G**, (b) **SG**, and (c) **N** catalysts. Open circles are $\bar{M}_n$ from GPC. The closed symbols are M_n^{NMR} from ^{1}H NMR, assuming each polymer chain to be end-capped by two terminal double bonds. Triangles represent the degree of isomerization as determined by ^{1}H NMR studies.

This can be understood as the cis configuration introducing kinks in the aliphatic sections of polymer chain, reducing the stability of the nematic phase. In contrast, the influence of isomerization (before coupling) on the transition temperatures is much more complicated, since isomerization could have effects on both the length of the flexible spacer as well as the position of the double bonds along the chain. For example, in Scheme 4, the formation of a 7-carbon spacer by one-step isomerization followed by coupling is shown. At lower degrees of isomerization, the formation of spacers containing seven methylene groups is most likely, so the tendency would be toward a lowering of the transition temperatures according to the "odd−even effect".[8,36] This is consistent with the observations on **SG**-catalyzed polymers that have significant isomerization and relatively low clearing temperatures. However, in comparing the two polymers with close molecular weight, P5tB-G2 and P5tB-N2, the polymer with *higher* isomerization (**N**, P5tB-N2) has a higher clearing temperature. This can only be explained by a dominating influence of trans content on clearing temperature.

(v) Kinetics Study of Polymerization and Isomerization. Dinger reported that the degradation product of **G** catalyst in the presence of methanol was, itself, an efficient catalyst for isomerization reactions.[37] Since we previously observed isomerization in the presence

of **G** catalyst, it is unclear whether the catalyst itself, or its degradation product, was responsible for isomerization; therefore, we studied the kinetics of both polymerization and isomerization reactions that would reveal the cause of isomerization. For this purpose, polymerizations were conducted with identical preparations including 0.5 g of monomer in 2 mL of toluene and [5tB]/[catalyst] = 55.55. The polymerization reactions were sampled at five different times under an inert atmosphere, with sampling times including 2, 6, 22, 44, and 66 h. We note that the polymerization conditions here are different than the varied conditions used for polymers in Table 1 and, therefore, not directly comparable. After vacuum-drying the samples at 50 °C, ^{1}H NMR (yielding isomerization and $\bar{M}_n^{NMR}$) and GPC (yielding $\bar{M}_n$) characterizations were performed for each sampling time.

Figure 7a shows the results for **G** catalyst. Interestingly, ^{1}H NMR, assuming $f = 2$ for the end-group analysis, indicates continued molecular weight increase with time until 22 h, whereas GPC indicates a molecular weight plateau after only 2 h of reaction. This apparent inconsistency is explained by the existence of isomerization: as shown in Scheme 4, the terminal double bonds could transform to internal ones by isomerization. In this scenario, the value of f decreases and, therefore, yields a false increase in the molecular weight when measured in this manner. From the GPC molecular weight data, it appears that after 2 h of reaction the **G** catalyst becomes inactive with respect to coupling reactions; i.e., the molecular weight does not increase any longer. Nevertheless, the degree of isomerization still increases, even after deactivation of the catalyst, indicating that the degradation product is capable of catalyzing isomerization. Similar findings were reported by Dinger.[31]

In the case of **SG** and **N** catalysts (parts b and c of Figure 7, respectively), ^{1}H NMR peaks of terminal double bonds cannot be discerned in most of the samples due to extensive isomerization, thus we only examined the time evolution of $\bar{M}_n$ from GPC and isomerization degree from ^{1}H NMR. The $\bar{M}_n$ show that, in contrast to **G** ADMET, molecular weight increases only gradually, reaching a plateau after a reaction time of about 22 h. On the other hand, the isomerization degree remains a constant high value of ~30% over the entire duration of the experiment, suggesting that all of the isomerization occurs within the first 2 h of the reaction and certainly involves the nondegraded **SG** catalyst, unlike the case for **G** catalyst. The behavior of the **N** catalyst (Figure 7c) is similar to that of **G** in that the isomerization rate increases as polymerization rate decreases, although at later times (>6 h) than for **G**. Thus, we speculate that Nolan's catalyst itself is responsible for the early 10% isomerization that occurs in the first 6 h but that the late-stage isomerization is catalyzed by a degradation product of the catalyst that is incapable of catalyzing polymerization.

When reaction conditions were held constant (unlike Table 1), clear trends in the effects of catalyst on the molecular weight and degree of isomerization were revealed. In particular, both the **N** and **SG** catalyst lead to high $\bar{M}_n$ of about 30 kDa, while the **G** catalyst leads to only 5 kDa. Thus, based on the molecular weight each catalyst could achieve, we conclude the order of the activity of these three catalysts in our ADMET polymerization system to be **N** (31.8 kDa) ≈ **SG** (24.7 kDa) > **G** (5.8 kDa). For long reaction times, reaching steady state, the overall selectivity against the isomerized structures of these three catalysts is **G** (87%) > **N** (82%) > **SG** (71%), a result consistent with earlier findings.[31−34] Indeed, the same ranking is observed independent of the reaction stage.

Conclusions

In this paper, the method of ADMET polymerization has been applied to the preparation of new unsaturated liquid crystalline polyesters based on a newly synthesized monomer, 2-*tert*-butyl-1,4-phenyl bis(4-pentenyloxybenzoate). Molecular weights, $\bar{M}_n$, in excess of 20 kDa were achievable, and the phase behavior and microstructural analysis indicated polymer-like characteristics. The polymerization products were robust, as indicated by significant molecular weight advancement that occurred on repeating the polymerization reaction in a fresh catalyst solution. It was found that the thermal transitions of the polymers (T_g and T_{NI}) strongly depend on the catalyst employed. Furthermore, detailed NMR investigations revealed the primary role of the trans/cis ratio and the secondary role of the isomerization degree in determining the observed nematic-to-isotropic transitions. Among the catalysts studied, Nolan's catalyst (**N**) yielded the highest fraction of trans double bonds within the spacers units and also the highest clearing transition. Kinetic studies of the polymerization and isomerization allowed us to prove that the degradation product of the Grubbs catalyst (**G**) is primarily responsible for late-stage isomerization reactions, while the second-generation Grubbs catalyst (**SG**) promotes isomerization in its nondegraded form. Nolan's catalyst was found to be active toward isomerization in both polymerization-active and deactivated forms. The unsaturated liquid crystalline polymers prepared in this study may serve as model TLCPs, based on their broad nematic phases (>100 °C) and sharp clearing transitions, and as liquid crystalline thermosets upon cross-linking of the residual carbon−carbon double bonds present in each repeat unit.

Acknowledgment. P.T.M. acknowledges AFOSR (F49620-00-1-0100) and NSF (CTS-00093880) and E.B.C. acknowledges NSF-Sponsored Material Research Science and Engineering Center on Polymers at UMass Amherst (DMR-0213695) for financial support of the research. We thank Prof. Nolan of University of New Orleans for kindly supplying catalyst **N**.

References and Notes

(1) Jackson, W. J., Jr.; Kuhfuss, H. F. *J. Polym. Sci., Polym. Chem. Ed.* **1976**, *14*, 2043−2058.
(2) Roviello, A.; Sirigu, A. *J. Polym. Sci., Polym. Lett. Ed.* **1975**, *13*, 455−463.
(3) Griffin, A. C.; Havens, S. J. *J. Polym. Sci., Polym. Phys. Ed.* **1981**, *19*, 951.
(4) Antoun, S.; Lenz, R. W.; Jin, J. I. *J. Polym. Sci., Polym. Chem. Ed.* **1981**, *19*, 1901−1920.
(5) Ober, C.; Jin, J. I.; Lenz, R. W. *Polym. J. (Tokyo)* **1982**, *14*, 9−17.
(6) Mather, P.; Grizzuti, N.; Heffner, G.; Ricker, M.; Rochefort, W. E.; Seitz, M.; Schmidt, H.-W.; Pearson, D. S. *Liq. Cryst.* **1994**, *17*, 811−826.
(7) Percec, V.; Yourd, R. *Macromolecules* **1989**, *22*, 524−537.
(8) Sirigu, A. In *Liquid Crystallinity in Polymers. Principles and Fundamental Properties*; Cifferi, A., Ed.; VCH Publishers: New York, 1991.
(9) Shiota, A.; Ober, C., K. *Prog. Polym. Sci.* **1997**, *22*, 975−1000.

(10) Lindmark-Hamberg, M.; Wagener, K. B. *Macromolecules* **1987**, *20*, 2949−2951.
(11) Wagener, K. B.; Nel, J. G.; Konzelman, J.; Boncella, J. M. *Macromolecules* **1990**, *23*, 5155−5157.
(12) Wagener, K. B.; Boncella, J. M.; Nel, J. G. *Macromolecules* **1991**, *24*, 2649−2657.
(13) Wagener, K. B.; Brzezinska, K. *Macromolecules* **1991**, *24*, 5273−5277.
(14) Patton, J. T.; Wagener, K. B. *Polym. Prepr. (Am. Chem. Soc., Div. Polym. Chem.)* **1992**, *33*, 1068−1069.
(15) Wagener, K. B.; Patton, J. T. *Macromolecules* **1993**, *26*, 249−253.
(16) O'Gara, J. E.; Portmess, J. D.; Wagener, K. B. *Macromolecules* **1993**, *26*, 2837−2841.
(17) Smith, D. W., Jr.; Wagener, K. B. *Macromolecules* **1993**, *26*, 1633−1642.
(18) Allcock, H. R.; Kellam, E. C., III; Hofmann, M. A. *Macromolecules* **2001**, *34*, 5140−5146.
(19) Allcock, H. R.; Kellam, E. C., III *Macromolecules* **2002**, *35*, 40−47.
(20) Walba, D. M.; Keller, P.; Shao, R.; Clark, N. A.; Hillmyer, M.; Grubbs, R. H. *J. Am. Chem. Soc.* **1996**, *118*, 2740−2741.
(21) Joo, S.-H.; Yun, Y.-K.; Jin, J.-I.; Kim, D.-C.; Zin, W.-C. *Macromolecules* **2000**, *33*, 6704−6712.
(22) Brzezinska, K.; Wagener, K. B. *Macromolecules* **1992**, *25*, 2049−2052.
(23) Rousseau, I. A.; Qin, H.; Mather, P. T. Manuscript in preparation.
(24) Maynard, H. D.; Grubbs, R. H. *Tetrahedron Lett.* **1999**, *40*, 4137−4140.
(25) Odian, G. *Principles of Polymerization*, 3rd ed.; Wiley-Interscience: New York, 1991.
(26) Qin, H.; Chakulski, B. J.; Mather, P. T.; Constable, G. S.; Coughlin, B. E. *Polym. Prepr. (Am. Chem. Soc., Div. Polym. Chem.)* **2003**, *44*, 40−41.
(27) Kim, S. S.; Han, C. D. *Macromolecules* **1993**, *26*, 6633−6642.
(28) Salvini, A.; Frediani, P.; Piacenti, F. *J. Mol. Catal. A: Chem.* **2000**, *159*, 185−195.
(29) Salvini, A.; Piacenti, F.; Frediani, P.; Devescovi, A.; Caporali, M. *J. Organomet. Chem.* **2001**, *625*, 255−267.
(30) Calderon, N.; Morris, M. C. *J. Polym. Sci., Polym. Phys. Ed.* **1967**, *5*, 1283−1292.
(31) Dinger, M. B.; Mol, J. C. *Adv. Synth. Catal.* **2002**, *344*, 671−677.
(32) Fuerstner, A.; Thiel, O. R.; Ackermann, L.; Schanz, H.-J.; Nolan, S. P. *J. Org. Chem.* **2000**, *65*, 2204−2207.
(33) Bourgeois, D.; Pancrazi, A.; Nolan, S. P.; Prunet, J. *J. Organomet. Chem.* **2002**, *643−644*, 247−252.
(34) Lehman, S. E.; Schwendeman, J. E.; O'Donnell, P. M.; Wagener, K. B. *Inorg. Chim. Acta* **2003**, *345*, 190−198.
(35) Selectivity was reported to depend on the reaction conditions and the structure of the initial olefins.
(36) Chang, S.; Han, C. D. *Macromolecules* **1997**, *30*, 1670−1684.
(37) Dinger, M. B.; Mol, J. C. *Organometallics* **2003**, *22*, 1089−1095.

MA0497456